

# Pseudorandom encoding for real-valued ternary spatial light modulators

Markus Duelli and Robert W. Cohn

Pseudorandom encoding with quantized real modulation values encodes only continuous real-valued functions. However, an arbitrary complex value can be represented if the desired value is first mapped to the closest real value realized by use of pseudorandom encoding. Examples of encoding real- and complex-valued functions illustrate performance improvements over conventional minimum distance mapping methods in reducing peak sidelobes and in improving the uniformity of spot arrays. © 1999 Optical Society of America

OCIS codes: 230.6120, 090.1760, 030.6600.

## 1. Introduction

Complex-valued spatial light modulators (SLM's) greatly simplify the design of transmittance functions for multispot beam steering systems and other Fourier-transform processors. With arbitrary complex modulation, many desired patterns can be specified with standard Fourier-transform tables. However, fully complex SLM's either are not widely available or are rather involved to construct.<sup>1</sup> For these reasons encoding methods are often used to approximate fully complex operation.<sup>2-4</sup> In adaptive or rapidly updated systems encoding may be preferred to global optimization methods<sup>5</sup> because of its speed. Because current SLM's have relatively low numbers of pixels compared with diffractive optics and holograms, methods that use group-oriented encoding<sup>6,7</sup> are undesirable in that they further reduce the useful space-bandwidth product. Two general methods that avoid grouping are pseudorandom encoding<sup>8</sup> (PRE) and minimum distance encoding<sup>9</sup> (MDE). Both methods map each desired complex value to a realizable modulation value of each corresponding SLM pixel. Most recently these methods have been evaluated and compared for SLM's that produce at least three quantized phase-only values.<sup>10</sup>

For the case of real-valued ternary modulation (i.e.,

SLM's that produce the modulation values of 1, 0, and  $-1$ ) it is not immediately evident that PRE can support fully complex representations. The problem is that the range of values that can be encoded is limited to real values between  $-1$  and  $1$  [Fig. 1(a)]. MDE is not limited to the real axis, since MDE maps the desired complex value to the closest modulation value. As shown in Fig. 1(b) MDE divides the complex plane into distinct regions. Any complex value in a given region is mapped to the single modulation value in that region. However, we have noted for other types of SLM that the accuracy with which the diffraction patterns approximate the desired diffraction patterns can be improved on by use of other types of encoding.<sup>10,11</sup>

The greatest improvement observed has been by use of a hybrid encoding algorithm that blends PRE with a modified MDE algorithm.<sup>12</sup> In this method the desired complex value is mapped to the closest value that can be produced by PRE. The mapped value is then pseudorandom encoded to produce the modified minimum distance PRE (mMD-PRE). This type of encoding is illustrated for the ternary SLM in Fig. 1(c). The mMD-PRE is a specific variant of PRE that permits complex-valued representation, even with the real-valued ternary SLM. The mMD-PRE can be contrasted with conventional minimum distance-PRE (MD-PRE). For the ternary SLM all values would be encoded by use of MDE [as in Fig. 1(b)] except those real values between  $-1$  and  $1$ , which would be encoded by PRE [as in Fig. 1(a)]. For typical complex-valued functions a negligible number of values would be encoded by PRE, and therefore the algorithm can be

---

The authors are with the ElectroOptics Research Institute, University of Louisville, Louisville, Kentucky 40292. R. W. Cohn's e-mail address is rwcohn01@ulkyvm.louisville.edu.

Received 22 January 1999; revised manuscript received 22 March 1999.

0003-6935/99/173804-06\$15.00/0

© 1999 Optical Society of America

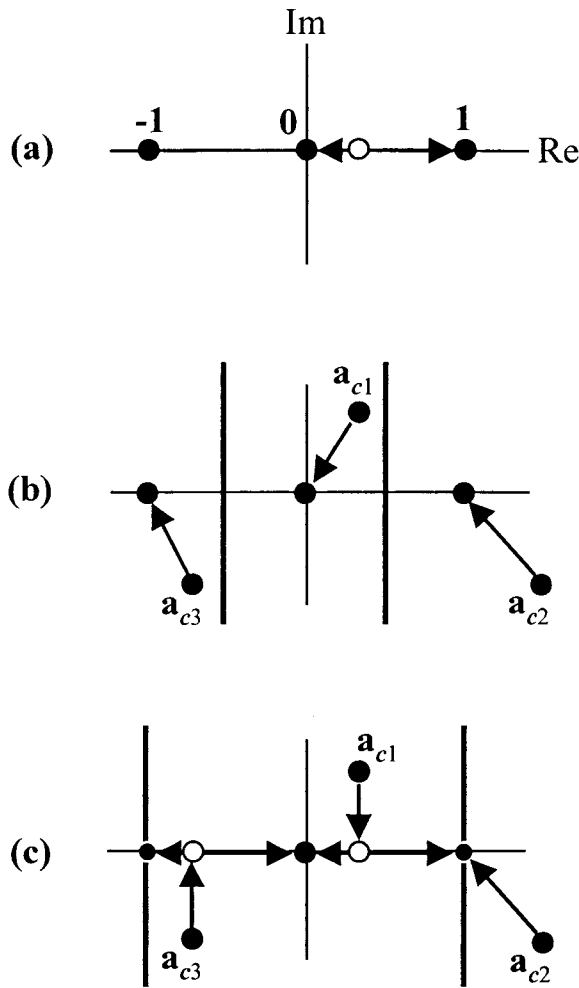


Fig. 1. Pixel-oriented encoding methods: (a) PRE, (b) MDE, (c) mMD-PRE. Method (c) also describes MD-PRE if the desired function is strictly real.

viewed essentially as being MDE. Two SLM's that produce such real ternary modulation are magneto-optic SLM's and analog chiral smectic liquid-crystal SLM's.<sup>13,14</sup>

Our objectives in this paper are (1) to demonstrate the feasibility of complex-valued representation by use of mMD-PRE with a real-valued ternary modulation characteristic, (2) to demonstrate the improvements over MDE alone, and (3), for the encoding of a strictly real function, to show the improvements of MD-PRE over MDE. These encoding algorithms also illustrate in brief the same general characteristics and performance trends that were reported for the application of these methods to various quantized phase SLM's in Ref. 12.

The paper is organized as follows: We present the various encoding algorithms; review definitions of the metrics used to compare them; and then compare the encoding algorithms, using computer simulations of two spot array generator designs (one in which the desired function is strictly real and the other in which the desired function is complex.)

## 2. Description of the Encoding Algorithms

### A. Minimum Distance Encoding

The MDE algorithm maps each desired complex value  $\mathbf{a}_{ci}$  (where  $i$  is the pixel index) to the closest available value ( $-1, 0,$  or  $1$ ) of the SLM. As illustrated in Fig. 1(b), the complex plane is divided into three decision regions. This mapping can be expressed as

$$\mathbf{a}_i = \begin{cases} \text{sgn}[\text{Re}(\mathbf{a}_{ci})] & \text{if } \frac{1}{2} \leq |\text{Re}(\mathbf{a}_{ci})|, \\ 0 & \text{if } |\text{Re}(\mathbf{a}_{ci})| < \frac{1}{2}, \end{cases} \quad (1)$$

The performance of the resulting diffraction pattern from this transmittance function can depend greatly on the scaling of the desired function  $\mathbf{a}_{ci}$ . The scaling can be written as

$$\mathbf{a}_{ci} = \gamma \exp(j\beta) \mathbf{a}'_{ci}, \quad (2)$$

where the maximum magnitude of  $\mathbf{a}'_{ci}$  for  $i = 1-N$  is unity. It is typical to optimize the performance metric of interest as a function of the two parameters  $\gamma$  and  $\beta$ . These parameters are also used for the same purpose in the blended algorithms considered here.

### B. Pseudorandom Encoding

PRE is a statistically based method of encoding in which one modulation value from a range of possible values is selected with a computer-generated random (i.e., pseudorandom) number. The statistical properties of the random-number generator are designed so that the average modulation value is identical to the desired complex value [see Eq. (1) in Ref. 10]. The diffraction pattern produced when we encode the values  $\mathbf{a}_{ci}$  of the desired transmittance function has an average intensity that is identical to the desired diffraction pattern plus a noise background. Additional theory and algorithm derivation procedures for a wide variety of modulator characteristics were presented in Refs. 15–17.

### C. Modified Blended Encoding

Following the two procedures above, we directly state the mMD-PRE algorithm. Any desired value found on the real axis between  $-1$  and  $1$  is encoded by PRE [Fig. 1(a)]. Desired values that have real parts that lie between  $-1$  and  $1$  are projected to the closest point on the real axis, and then the projected value is encoded by PRE [Fig. 1(c)]. Values that have real values that are greater than  $1$  or less than  $-1$  map to the closest available modulation values  $1$  and  $-1$ , respectively. The mathematical specification of the encoding algorithm associates a probability with the desired value  $\mathbf{a}_{ci}$  according to

$$p = |\text{Re}(\mathbf{a}_{ci})|. \quad (3)$$

With this value of probability the encoding formula is

$$\mathbf{a}_i = \begin{cases} \text{sgn}[\text{Re}(\mathbf{a}_{ci})] & \text{if } 0 \leq s_i < p_i \quad \text{or } 1 < p_i, \\ 0 & \text{if } p_i \leq s_i \leq 1, \end{cases} \quad (4)$$

where  $\mathbf{a}_i$  is the actual modulation selected for the  $i$ th modulator pixel and  $s_i$  is a pseudorandom number selected from the uniform distribution with mean 0.5 and a spread of unity. Equation (4) shows that the closer the real part is to an actual modulation value the more frequently that value is selected. For cases in which the real magnitudes exceed unity,  $p_i$  cannot be considered to be a probability and random selection cannot be used. Instead MDE is used that corresponds to the first line of Eq. (4) when the second part of the if statement is true. Also note that, if the desired function is strictly real, then Eqs. (3) and (4) also describe MD-PRE. That is, the real values between  $-1$  and  $1$  are encoded by PRE, and the values with magnitudes greater than unity are encoded by MDE. In this study both strictly real and fully complex desired functions were encoded, which permits comparisons of mMD-PRE with MDE and PRE individually and comparisons of MD-PRE with MDE and PRE individually.

### 3. Design of Simulation Experiments

The real-valued and the fully complex desired functions are designed to produce a  $7 \times 7$  array of uniform intensity spots in the diffraction plane. They are based on the functions reported in Tables 1 and 3 of Krackhardt *et al.* for  $1 \times 7$  spot arrays.<sup>18</sup> Their functions on conversion to biamplitude ( $1, -1$ ) and analog phase-only functions have the highest possible diffraction efficiency (their transform from desired function to realizable modulation is equivalent to MDE with  $\gamma = \infty$ ). Our two desired functions are two-dimensional rectangularly separable functions that are constructed when we cross their one-dimensional functions. The function is sampled to produce a  $128 \times 128$  pixel matrix that consists of a  $4 \times 4$  array of unit cells. Additionally, a phase ramp is added to the fully complex function so that it reconstructs off axis. The phase ramp makes the encoded function essentially independent of the phase parameter  $\beta$ . Therefore only  $\gamma$  is varied in the evaluation of the encoding algorithms. For purposes of evaluating the encoding algorithms with real-valued functions, again, only  $\gamma$  is varied.

The key metrics of interest describe the accuracy (or fidelity) with which the actual reconstruction matches that for the desired function. These are the nonuniformity (NU) of the spot array, which is calculated as the standard deviation of the peak intensities of the 49 spots divided by the average intensity of the spots, and the signal-to-peak-noise ratio (SPR), which is the ratio of the average peak intensity of the spots to the maximum noise peak found in the diffraction pattern (excluding the square region that contains the  $7 \times 7$  spot array). We feel that these metrics are especially important in real-time systems for which it is not practical to perform designs on the fly with numerically intensive optimization.

It is also common to report diffraction efficiency  $\eta$  for most designs. We can calculate this by first summing the intensities of the 49 spots, dividing by the sum of all intensities in the diffraction pattern, and then mul-

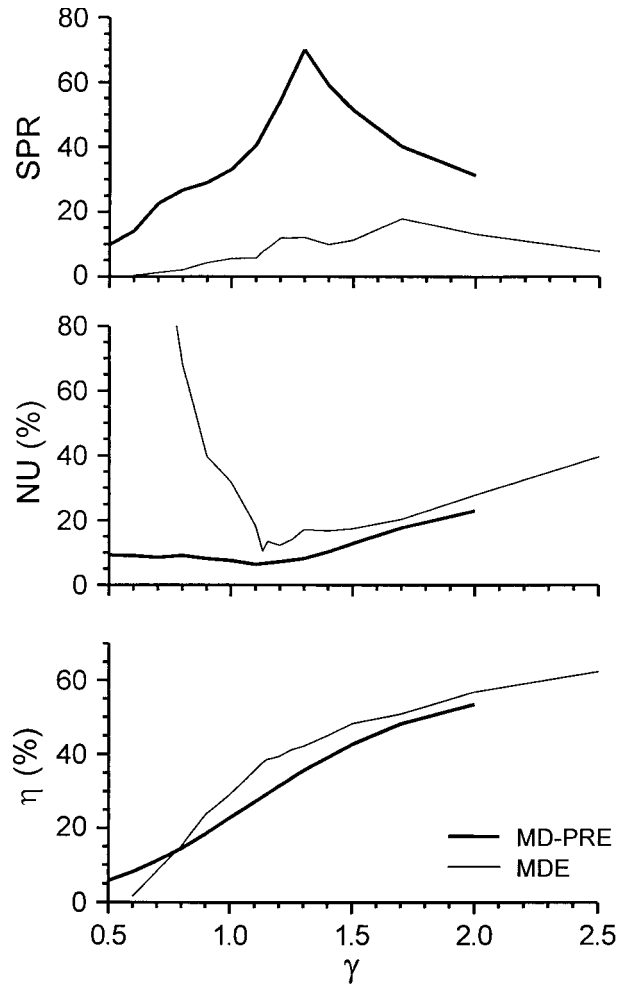


Fig. 2. Performance of MDE and MD-PRE as a function of the magnitude scaling parameter for encoding the real-valued function.

tiplying this by an additional factor that accounts for the absorption by the zero-valued modulation states. This factor is simply the ratio of the unity magnitude values divided by the total number of SLM pixels. We will show that there is a continuous trade-off between fidelity and diffraction efficiency and the best fidelity is achieved when the diffraction efficiency is less than the maximum possible.

### 4. Comparison of the Encoding Methods

Figure 2 shows how the performance of encoding the

Table 1. Performance for Encoding the Real-Valued Function

Encoding	$\gamma$	$\eta$ (%)	SPR	NU (%)
MD-PRE <sup>a</sup>	1.1	27	41	6.3
MDE <sup>a</sup>	1.13	38	7.9	10.4
MD-PRE <sup>b</sup>	1.3	36	70	8.1
MDE <sup>b</sup>	1.7	51	18	20.3
MDE	$\infty$	73	5.1	45.0

<sup>a</sup>Minimum NU.

<sup>b</sup>Maximum SPR.

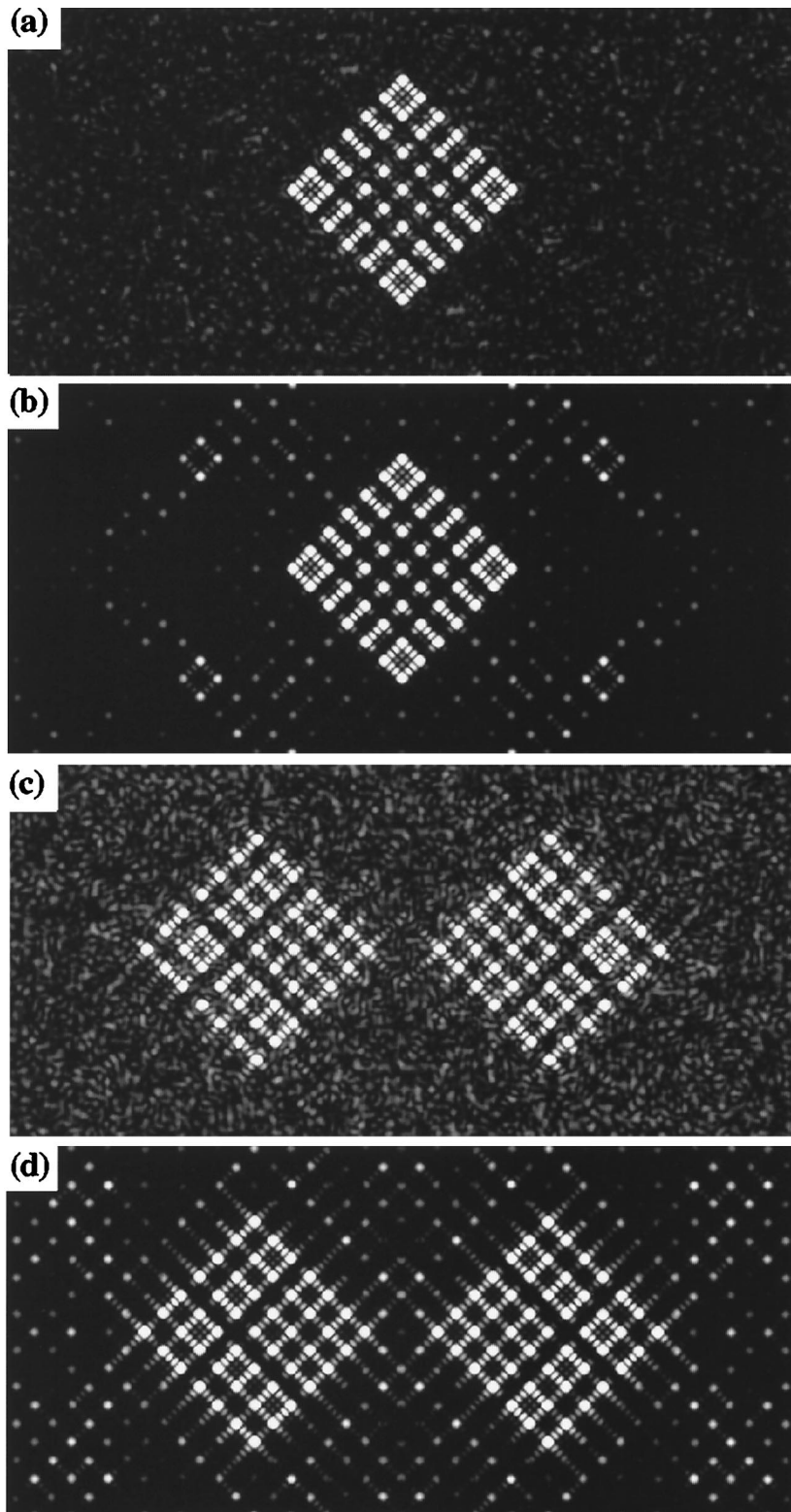


Fig. 3. Diffraction patterns for (a) MD-PRE for  $\gamma = 1.1$  and (b) MDE for  $\gamma = 1.13$  for the real-valued desired function and (c) mMD-PRE for  $\gamma = 1.05$  and (d) MDE for  $\gamma = 1.9$  for the complex-valued desired function. The intensity images are saturated so that the full white gray scale corresponds to  $\frac{1}{10}$  of the average intensity of the 49 spots. Also, the images are shown rotated by  $45^\circ$  from the  $x$ - $y$  coordinate system.

real-valued function by use of MDE and MD-PRE depends on the parameter  $\gamma$ . For both encoding algorithms the largest value of SPR and the smallest

value of NU are found for  $\gamma$  somewhat greater than unity. MD-PRE always achieves significantly larger values of SPR and somewhat smaller values of

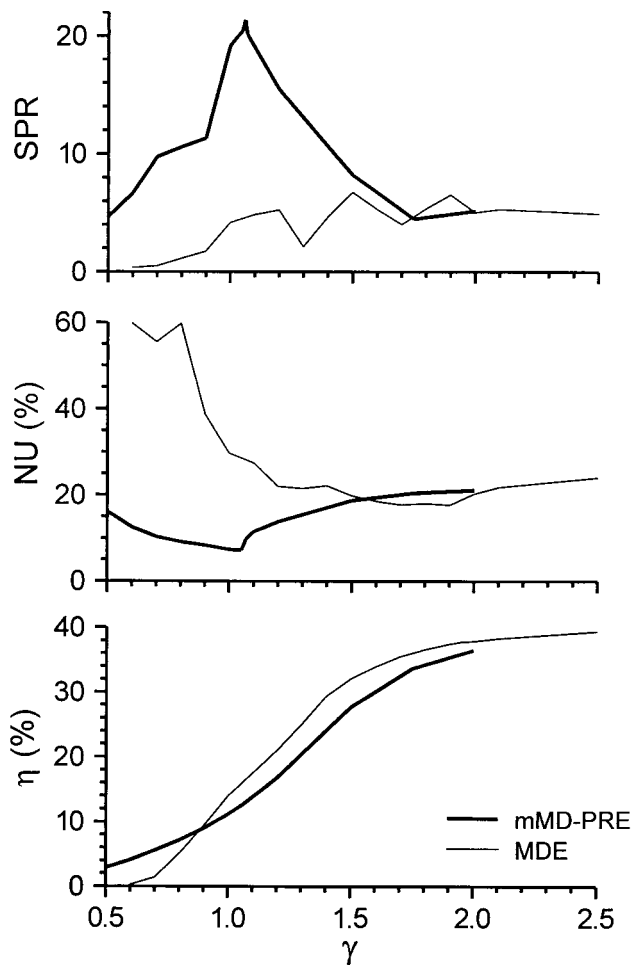


Fig. 4. Performance of MDE and mMD-PRE as a function of the magnitude scaling parameter for encoding the complex-valued function.

NU than does the MDE. These trends and observations are in agreement with those reported in Ref. 12 for various multiphase SLM's. The trends are further brought out in Table 1, which reports the performance for each algorithm when NU is minimum and when SPR is maximum. The table also compares these results with MDE for  $\gamma = \infty$  (i.e., the Krackhardt *et al.* biamplitude design). Clearly, the fidelity is much improved by a trade-off of the diffraction efficiency.

Figures 3(a) and 3(b) show a portion of the computer-simulated on-axis diffraction pattern for the MD-PRE and MDE designs reported in Table 1 for minimum NU. Although speckle noise is evident

Table 2. Performance for Encoding the Complex-Valued Function

Encoding	$\gamma$	$\eta$ (%)	SPR	NU (%)
mMD-PRE <sup>a</sup>	1.05	12	20.4	7.2
MDE <sup>a</sup>	1.90	37	6.5	17.6
MDE	$\infty$	40	5.3	26.1

<sup>a</sup>Minimum NU.

throughout the image of the MD-PRE encoding, there are no significant noise spikes. In Fig. 3(b) most of the background area is pure black; however, there are a number of noise spikes that are quite bright and evident. These noise spikes are due to the inherent nonlinearity of mapping from the continuous real-valued function to the three-valued quantized modulator. The systematic method of mapping in MDE induces strong harmonic terms at sum and difference frequencies of the desired modulation. MD-PRE tends to reduce this effect by distributing noise energy more uniformly over the entire diffraction plane.

Figure 4 presents the performance of encoding the fully complex function by MDE and mMD-PRE as a function of  $\gamma$ . The same sort of trends are seen as a function of  $\gamma$  and in comparing MDE with mMD-PRE as were seen in comparing MDE with MD-PRE. The performance metrics for each algorithm are reported in Table 2. The minimum NU metrics are reported, since they differ only slightly with the maximum SPR design.

The simulated diffraction patterns for the minimum NU design mMD-PRE and MDE designs are given in Figs. 3(c) and 3(d), respectively. Because the SLM can produce only real values and the design produces an off-axis reconstruction, there is a mirror symmetry in both diffraction patterns. Again mMD-PRE has higher SPR than MDE, owing to its distributing the noise over the entire diffraction plane. Comparing Fig. 4 with Fig. 2, we see that the SPR and the diffraction efficiency are substantially smaller in Fig. 4. This is primarily a result of the energy being divided between the desired and the mirror order. The reduction in SPR is also evident when we compare Figs. 3(a) and 3(b) with Figs. 3(c) and 3(d), where the background noise is more evident. However, even with much reduced diffraction efficiency, good performance is possible. As long as the mirror image is acceptable, it appears that a ternary SLM can do a good job of multispot beam steering. Much better performance would be possible with traditional diffractive optical element design approaches. This would involve reoptimizing the design even if the spot array were simply steered to a new location. Such operations would be extremely cumbersome and would limit the adaptivity of many real-time SLM-based systems.

## 5. Conclusions

In this paper we extend and reinforce the results originally made in Ref. 12, using quantized phase SLM's. For purposes of producing a Fourier-transform hologram from a desired fully complex-valued function the most faithful encoding method (as measured by SPR and NU) is modified-minimum-distance-pseudorandom encoding (mMD-PRE). Though there is a mirror image for off-axis reconstructions, the real-valued ternary SLM can represent complex-valued functions with good fidelity and moderate diffraction efficiency by use of the mMD-PRE algorithm. The ability to represent complex values on SLM's of such extremely limited mod-

ulation is especially useful for reducing the time and cost of prototyping SLM's and SLM-based systems.

This study was supported by Office of Naval Research grant N00014-96-1-1296 and NASA cooperative agreement NCC5-222.

## References

1. L. G. Neto, D. Roberge, and Y. Sheng, "Full-range, continuous, complex modulation by the use of two coupled-mode liquid-crystal televisions," *Appl. Opt.* **35**, 4567-4576 (1996).
2. D. C. Chu, J. R. Fienup, and J. W. Goodman, "Multiemulsion on-axis computer generated hologram," *Appl. Opt.* **12**, 1386-1388 (1973).
3. B. R. Brown and A. W. Lohmann, "Complex spatial filter," *Appl. Opt.* **5**, 967 (1966).
4. R. W. Cohn and L. G. Hassebrook, "Representations of fully complex functions on real-time spatial light modulators," in *Optical Information Processing*, F. T. S. Yu and S. Jutamulia, eds. (Cambridge University, Cambridge, UK, 1998), Chap. 15, pp. 396-432.
5. J. N. Mait, "Diffractive beauty," *Opt. Photon. News* **52**, 21-25 (1998).
6. W.-H. Lee, "Computer-generated holograms: techniques and applications," in *Progress in Optics*, E. Wolf, ed. (Elsevier, Amsterdam, 1978), Vol. 16, pp. 119-231.
7. W. J. Dallas, "Computer-generated holograms," in *The Computer in Optical Research*, B. R. Frieden, ed. (Springer-Verlag, Berlin, 1980), Chap. 6, pp. 291-366.
8. R. W. Cohn, "Pseudorandom encoding of fully complex functions onto amplitude coupled phase modulators," *J. Opt. Soc. Am. A* **15**, 868-883 (1998).
9. R. D. Juday, "Optimal realizable filters and the minimum Euclidean distance principle," *Appl. Opt.* **32**, 5100-5111 (1993).
10. R. W. Cohn and Markus Duelli, "Ternary pseudorandom encoding of Fourier transform holograms," *J. Opt. Soc. Am. A* **16**, 71-84 (1999).
11. L. G. Hassebrook, M. E. Lhamon, R. C. Daley, R. W. Cohn, and M. Liang, "Random phase encoding of composite fully complex filters," *Opt. Lett.* **21**, 272-274 (1996).
12. M. Duelli, M. Reece, and R. W. Cohn are preparing a manuscript to be called "Modified minimum distance criterion for blended random and nonrandom encoding."
13. B. A. Kast, M. K. Giles, S. D. Lindell, and D. L. Flannery, "Implementation of ternary phase amplitude filters using a magneto-optic spatial light modulator," *Appl. Opt.* **28**, 1044-1046 (1989).
14. *VLSI Spatial Light Modulators*, Operations Manual for 128 x 128 analog SLM, revision 1.6 (Boulder Nonlinear Systems Inc., Lafayette, Colo., 1998).
15. R. W. Cohn and M. Liang, "Approximating fully complex spatial modulation with pseudorandom phase-only modulation," *Appl. Opt.* **33**, 4406-4415 (1994).
16. R. W. Cohn and M. Liang, "Pseudorandom phase-only encoding of real-time spatial light modulators," *Appl. Opt.* **35**, 2488-2498 (1996).
17. R. W. Cohn, "Analyzing the encoding range of amplitude-phase coupled spatial light modulators," *Opt. Eng.* **38**, 361-367 (1999).
18. U. Krackhardt, J. N. Mait, and N. Streibl, "Upper bound on the diffraction efficiency of phase-only fanout elements," *Appl. Opt.* **31**, 27-37 (1992).